clean technologies

MDPI

Article

Measurement and Correlation of Vapor–Liquid Equilibrium of Mixtures of 1,2-Propanediol or 1,4-Butanediol + 1,8-Diazabicyclo(5.4.0)undec-7-ene at 30 kPa

Camilla Barbieri [1], Valentina Schiattarella [1], Stefania Moioli [1,*], Laura A. Pellegrini [1], Giacomo Filippini [2], Alberto R. de Angelis [2] and Gianluca Fiori [2]

[1] GASP, Group on Advanced Separation Processes & GAS Processing, Dipartimento di Chimica, Materiali e Ingegneria Chimica "Giulio Natta", Politecnico di Milano, Piazza Leonardo da Vinci 32, I-20133 Milano, Italy
[2] Eni S.p.A. Research and Technological Innovation Department, Via F. Maritano 26, I-20097 San Donato Milanese, Italy
* Correspondence: stefania.moioli@polimi.it

Abstract: In this study, vapor–liquid equilibrium (VLE) experimental data were measured for two binary solvents based on 1,8-diazabicyclo(5.4.0)undec-7-ene (DBU), which can be used as a new CO_2-binding organic liquids (CO_2-BOLs) solvent. No experimental data are available in the literature and are fundamental to determine whether the considered mixtures are suitable to be possible alternatives to traditional amine solutions for CO_2 removal. The bubble point data of 1,2-propanediol+1,8-diazabicyclo(5.4.0)undec-7-ene (DBU) and 1,4-butanediol+DBU mixtures were measured at 30 kPa. The experimental determination was carried out in an all-glass dynamic recirculation still at the Process Thermodynamics laboratory (PT lab) of Politecnico di Milano. The thermodynamic modeling of the VLE behavior of two DBU-based mixtures was performed considering the NRTL, the UNIQUAC, and the Wilson models, and binary interaction parameters of the NRTL activity coefficients model were regressed on the basis of the measured experimental data.

Keywords: CO_2-BOLs; DBU; VLE data; PT lab

check for updates

Academic Editor: Shunde Yin

Received: 24 October 2024
Revised: 29 November 2024
Accepted: 25 December 2024
Published: 30 December 2024

Citation: Barbieri, C.; Schiattarella, V.; Moioli, S.; Pellegrini, L.A.; Filippini, G.; de Angelis, A.R.; Fiori, G. Measurement and Correlation of Vapor–Liquid Equilibrium of Mixtures of 1,2-Propanediol or 1,4-Butanediol + 1,8-Diazabicyclo(5.4.0)undec-7-ene at 30 kPa. *Clean Technol.* **2025**, *7*, 3. https://doi.org/10.3390/cleantechnol7010003

Copyright: © 2024 by the authors. Licensee MDPI, Basel, Switzerland. This article is an open access article distributed under the terms and conditions of the Creative Commons Attribution (CC BY) license (https://creativecommons.org/licenses/by/4.0/).

1. Introduction

The global CO_2 emissions have risen to the new all-time value in 2022 of 36.1 ± 0.3 $GtCO_2$, indicating that the pre-pandemic trend of continuous growth might have started again [1]. Hence, jointly boosting CO_2 capture technologies is mandatory in order to limit the anthropogenic warming to 1.5 °C above the pre-industrial levels, meeting the target set at the 25th UN Climate Change Conference of the Parties (COP25) in Paris in 2015.

The main CO_2 capture strategies from power plant exhausts are oxy-fuel combustion, precombustion, and post combustion [2]. Post combustion carbon capture (PCCC) can be implemented on the existing facilities after easy retrofitting, becoming the most efficient way for CO_2 emission mitigation in the short term [3,4]. Out of the many PCCC technologies, including membrane separation [5], adsorption-based processes (temperature swing, pressure swing, and vacuum swing) [6], physical and chemical absorption [7], and cryogenic separation [8], CO_2 capture by amine-based solvents is the most advanced separation technique, with a technology readiness level (TRL) higher than 9 [9]. In this respect, the aqueous 30% wt. monoethanolamine (MEA) solution is known to be the benchmark solvent because of its low cost and high reactivity [10], which enables high selectivity, fast absorption rate, large cyclic capacity, and high removal efficiency [4]. However, the

energy for the solvent regeneration is as high as about 4 GJ/ton CO_2, accounting for about 60–80% of the total energy consumed during CO_2 capture [11], and it is also related to the large amount of water that needs to be heated during the regeneration process. Moreover, MEA is well known to be toxic and corrosive towards column walls and pipelines [12], and it is subject to thermal and thermal-oxidative degradation at the desorption stage, leading to solvent losses, and converted to heat-stable salts (HSS), which can even reach 80 g of the 30% MEA solution per ton of absorbed CO_2 [13]. It has been estimated that in a 250 MW coal-fired thermal power plant (CO_2 emissions of 49 kg/s), the loss of absorbent (30% MEA solution) would be 120 tons per year of operation, which is about 10% from the initial content of MEA in solution [14]. For these reasons, developing new solvents that can efficiently capture CO_2 is crucial.

Starting from the breakthrough work by Jessop et al. [15], a new type of solvents made of amidine base and alcohol has attracted researchers' attention. These solvents, switchable ionic liquids (SILs) or CO_2-binding organic liquids (CO_2-BOLs), are able to switch from a non-polar, non-ionic liquid mixture (the alcohol plus the amidine base) to a polar, ionic liquid blend upon exposure to an atmosphere of carbon dioxide. One of the first developed SILs is DBU+1-hexanol. This mixture is characterized by a specific heat of 1.5 J/(g °C) [16], which is less than the half of the water-specific heat (4.18 J/(g °C) [17]), leading to an energy saving in the solvent regeneration step, when performed at temperatures comparable with those of the MEA process, of about 60% [16]. In addition, this blend, as any related to the Jessop's switchable solvents chemistry, fixates CO_2 as an alkylcarbonate species through a reaction pathway known from works by Heldebrant et al. [18,19] and recently further investigated by Wanderley et al. [20]. CO_2 binds more weakly in alkylcarbonate salts than in a bicarbonate and carbamate salts, as seen in conventional aqueous amine systems, at least partly because of the decreased hydrogen bonding (a free energy of binding of −9.4 kJ/mol was measured by Heldebrant [16] in the case of a 1,8-diazabicyclo(5.4.0)undec-7-ene (DBU)+1-hexanol mixture). The result is that less energy is required to thermally strip CO_2 from the liquid, and, for example, the carbon dioxide release in the DBU+1-hexanol system was measured to be nearly complete at 363.15 K [18]. The addition of a chemically inert non-polar antisolvent could further reduce this temperature, as shown in the case of the 1-((1,3-Dimethylimidazolidin-2-Ylidene)amino)propan-2-ol, whose regeneration temperature was reduced to 346.15 K by the addition of hexadecane [21]. This suggests that the stripping column could be run at a temperature lower than 393.15 K, the typical regeneration temperature of the MEA system. Zhu et al. (2020) [22] investigated the DBU+glycerol system and verified that it has a higher circulating CO_2 loading than MEA aqueous solution. Both DBU+glycerol solution and 30% wt. MEA were subjected to ten cycles of absorption–desorption experiments, and even though their original CO_2 loading was almost the same (2.98 $mol_{CO2}/kg_{\ absorbent}$ vs. 2.90 $mol_{CO2}/kg_{\ absorbent}$ respectively), the CO_2 loading at the 10th cycle was more than 90% of the initial loading for the DBU+glycerol system and just 60% for the MEA system. The absorption performances of this mixture were also studied by Duan et al. [23], and the rotating reactor was proposed as a valuable alternative to the traditional absorption column, which is not suitable for highly viscous solvents such as DBU+glycerol, whose viscosity can increase from 105.4 (DBU+glycerol solvent with 62.3 wt% DBU at 328.15 K) to 4443 mPa·s as the mass fraction of the absorbed CO_2 increases from 0 to 12.88 wt% [24]. Finally, Li et al. [25] focused on the same DBU+glycerol mixture, trying to enhance the CO_2 absorption and desorption rate through the addition of SiO_2 nanoparticles. They discovered that 16 nm SiO_2 nanoparticles can increase the CO_2 absorption rate by 31% compared with the base liquid (DBU+glycerol molar ratio 3:1 at 313.15 K), where this effect can be mainly ascribed to an increase in the interfacial area between the gas and liquid after the addition of the nanoparticles. Ternary systems

have also been investigated. By replacing part of DBU with 2-amino-2-methyl-1-propanol (AMP) in the DBU+ethanol system, a significantly reduced viscosity was obtained. For a CO_2 loading of 2.98 $mol_{CO2}/kg_{absorbent}$ at 313.15 K (achieved by the 50 wt% ethanol and equimolar DBU and AMP mixture), the viscosity was found to be 2.39 and 13.81 mPa·s, respectively, before and after CO_2 absorption [26], which is much lower than the viscosity change of many CO_2-BOLs. In the work by Hedayati et al. [27], it was found that the addition of tertiary alkanol amines to the two-component BOLs (DBU +alcohol) allows the synthesis of a pressure-sensitive solvent for a more efficient regeneration step, and moreover, for the first time, experimental CO_2 solubility data for DBU+n-butanol, DBU+dimethylethanolamine (DMEA), and DBU+DMEA+n-butanol were obtained in the temperature range of 298.15–318.15 K and the pressure range of 100–4500 kPa.

A detailed literature analysis on the vapor–liquid equilibrium (VLE) of the considered solvent and of mixtures with DBU was carried out in this study. Even though some papers in the literature on DBU-based CO_2-BOLs can be found, the VLE of pure DBU and its mixtures has been poorly investigated. Also, the vapor pressure of pure DBU was measured only by Ostonen et al. [28] between 375.77 K and 437.20 K and Lipkind et al. [29] between 328.2 K and 368.1 K, which shows this lack of knowledge. As far as the authors know, only the isothermal VLE of the binary DBU+H_2O was experimentally addressed in the temperature range 312.81–352.34 K [30]. No other sources of VLE data were found. The study of the thermodynamics of the solvent without CO_2 is fundamental in order to best characterize the mixture and to definitely establish it as a suitable solvent for CO_2 removal. For instance, a good solvent should be characterized by low vapor pressure, no presence of minimum boiling azeotropes, and a high difference in volatility with one of the gases to be absorbed. These characteristics can only be outsourced from VLE experimental data of mixtures, which are therefore needed for the evaluation of the suitability of a new solvent for CO_2 capture and, once the solvent is chosen, for the selection of the thermodynamic model to be employed for process simulation. Hence, the aim of this work was to measure the vapor–liquid equilibrium experimental data, i.e., bubble point data, of two binary systems (1,2-propanediol+DBU and 1,4-butanediol+DBU) that are considered of interest as new CO_2-BOLs, and to perform their thermodynamic modeling.

2. Materials and Methods

2.1. Materials Used

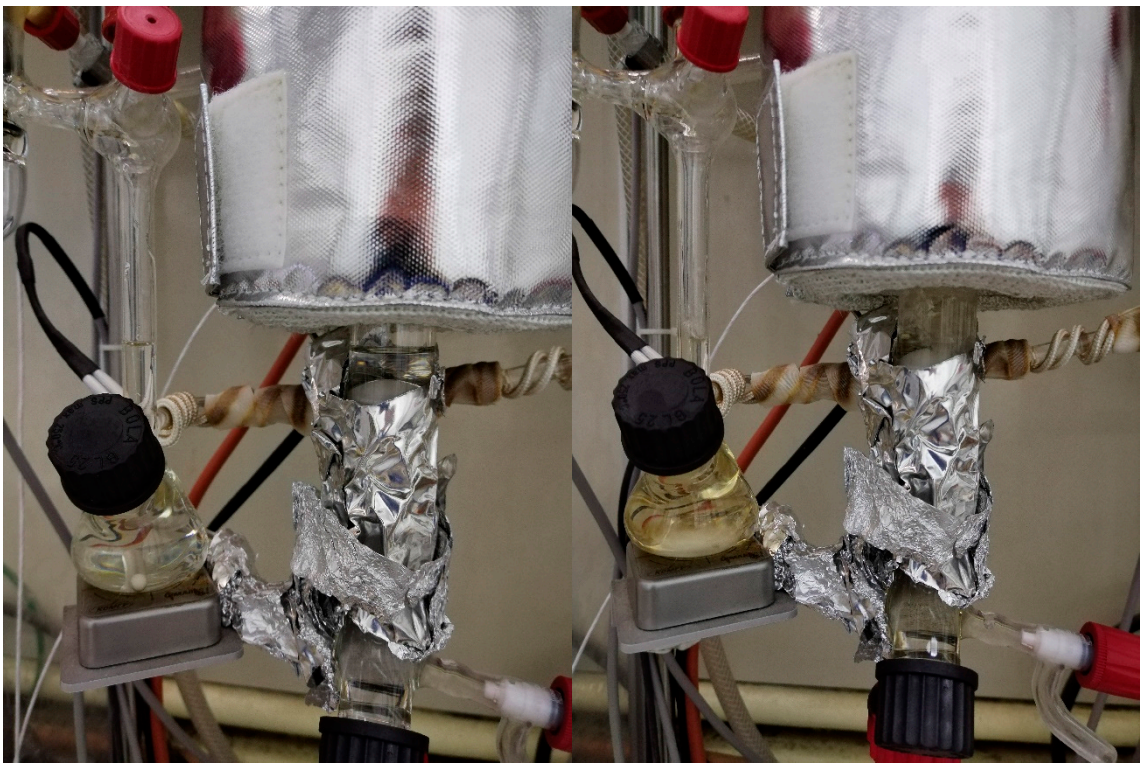
The chemicals used in this work are listed in Table 1. Gas chromatographic (GC) analyses for 1,2-propanediol and 1,4-butanediol were performed at the PT lab with the Agilent 7820A gas chromatograph equipped with a thermal conductivity detector (TDC) and a HP-INNOWAX stationary phase of 0.5 µm thickness to check their purity. The purity of DBU was not checked because of the corrosive nature of the DBU with respect to the metals, which constitute part of the internal apparatus of the GC, and detailed information on the composition of DBU was provided by the supplier. The reagents supplied by Sigma-Aldrich (Darmstadt, Germany) were then treated by distillation to increase their purities for obtaining a water content lower than 0.05% for 1,2-propanediol and 1,4-butanediol and lower than 0.1% for DBU for carrying out the experimental tests. The water content was checked by titration and, in the case of DBU, by additionally employing a buffer solution. Gaseous nitrogen (>99.99% mol.), supplied by Sapio, was used for the pressure control of the VLLE unit (Fischer® Labodest® VLLE 602, ILUDEST Destillationsanlagen GmbH, Waldbüttelbrunn, Germany) and as a carrier for the GC unit. Table 1 also details the density measured in this work with the densimeter Densito Density2Go by Mettler Toledo Technologies at a temperature of 292.15 K (indicated as "*Exp.*").

Table 1. Details of the chemicals from the supplier.

Component	CAS	Supplier	Purity (Mass Fraction)	Analysis Method	Density		Molecular Weight ($g \cdot mol^{-1}$)	T_{Nb} [°C]
					Lit. [a]	Exp.		
1,2-propanediol	57-55-6	Sigma-Aldrich	0.99	GC	1.036	1.0372	76.09	187 [a]
1,4-butanediol	110-63-4	Sigma-Aldrich	0.99	GC	1.017	1.0167	90.12	230 [a]
1,8-diazabicyclo(5.4.0)undec-7-ene (DBU)	6674-22-2	Sigma-Aldrich	0.98	GC	1.018	1.0190	152.24	261 [31]

[a] Safety Data Sheet by Sigma Aldrich.

The 98% wt. DBU is colorless, even at the start of the boiling, and it definitely turns into yellow throughout the VLE measurements, as reported in Figure 1. Ostonen et al. [28] observed the same behavior when DBU (purity $\geq$ 99% wt., the rest being mainly water) was distilled under 1 kPa pressure. Assuming that the change in the color is due to the presence of an impurity, its content would be very small and is considered to not significantly affect the measurements of the VLE of the mixtures.



(**a**) (**b**)

Figure 1. DBU (98% wt.) (**a**) loaded into the still at the beginning and (**b**) during the VLE measurements at the PT lab of Politecnico di Milano.

2.2. Experimental Apparatus

Politecnico di Milano is provided with the Process Thermodynamics laboratory (PT lab), which was created within the "Ingegneria Chimica—Energia (ICE)" collaboration and is located at Dipartimento di Chimica, Materiali e Ingegneria Chimica "Giulio Natta" [30,32,33].

An all-glass dynamic recirculation still (Fischer® Labodest® VLLE 602, Figure 2) coupled to a vacuum pump was used to measure the bubble point curve of the binary mixtures of interest. The detailed scheme of the unit is reported in Figure 1 of Barbieri et al. [34]. The unit, reported in Figure 2, contains a concentric electrical immersion heater (1), for supplying heat to the liquid mixture fed to the unit. Within the heating

chamber, a Pt-100 resistance thermometer (9) is used to measure the boiling temperature. Its accuracy and its resolution are, respectively, ±0.1 K and 0.01 K, as indicated by the supplier. The Cottrell pump (2) has the aim of ensuring that a very intensive heat and mass transfer occurs between the rising vapor and the boiling liquid, which enters into the separation chamber (3), where a second Pt-100 resistance thermometer (8) is used to measure the temperature at which the stationary behavior (vapor–liquid equilibrium, VLE) of the system is reached. Within the separation chamber, the vapor and liquid phases are split. The vapor phase is condensed, and both the liquid and the condensed vapor phases return to the mixing chamber (7), where the mixture is homogenized and then fed back again to the immersion heater chamber. The unit can be operated under vacuum conditions up to 400 kPa and up to a temperature of 523.15 K. The temperature range is higher than the base one characteristic of this unit because the optional high-temperature accessories, which include the heating mantle (20) to compensate heat losses and to avoid stress in the glass and the heating line (19) to avoid any blockings in the capillary tube, were installed. If the operating temperature is higher than 453.15 K, the temperature of the heated isolation jacket should be increased stepwise. As soon as both the liquid and condensate phases circulate in the unit, the set point of the heating mantle can be set to a value close to that shown by the Pt-100 (8). The FISCHER® [VLE] digital controller, whose pressure transmitter has an accuracy of ±100 Pa, as indicated by the supplier, is employed to set the heating element, the high-temperature accessories, and the operating pressure. The pressure sensor was calibrated just before the start of the experiments reported in this work.

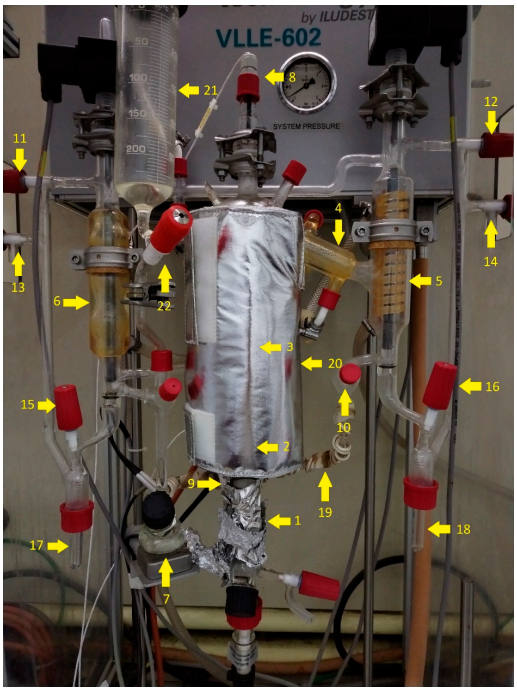


Figure 2. Schematic representation of the experimental setup: 1—heater, 2—Cottrell-pump, 3—separation chamber, 4—condenser, 5—safety cooler vapor phase, 6—safety cooler liquid phase, 7—mixing chamber with PTFE stirrer bar, 8—Pt-100 VLE temperature, 9—Pt-100 bubble point temperature, 10—dripping tip condensed vapor phase, 11—PTFE valve for pressure equilibrium to receiver No. 17, 12—PTFE valve for pressure equilibrium to receiver No. 18, 13—ventilation valve liquid sample, 14—ventilation valve vapor sample, 15—PTFE valve for liquid sample, 16—PTFE valve for vapor sample, 17—receiver for liquid sample, 18—receiver for vapor sample, 19—heating line, 20—heating mantle, 21—feed vessel and 22—PTFE valve at the feed vessel.

2.3. Experimental Procedure

In this work, the boiling curves were measured under vacuum conditions, at 30 kPa, because the VLE unit can operate up to 523.15 K, and the normal boiling point of the pure DBU is known to be 534.15 K, a temperature higher than the maximum operating temperature of the unit. A good solvent for CO_2 removal should be characterized by low volatility. This study is conservative because, by selecting a pressure lower than the atmospheric one (30 kPa), the temperatures at which the vapor phase may form at 30 kPa are lower than the ones at 101 kPa. If these temperatures are higher than the temperatures usually considered in the absorption process at pressures higher than 101 kPa, then it can be concluded that the solvent is not volatile and can be considered as a possible solvent for CO_2 removal. Accordingly, the vacuum pump was connected to the unit, and a 750 mL mixture of ice and alcohol (80% vol. and 20% vol., respectively) was charged into the Dewar, where the trap of the vacuum pump was placed in order to avoid the feed of any possible trace of condensate to the pump. The mixture (at least 240 mL) was prepared under the hood in a flask with a stopper (the sensibility of the balance is 0.001 g), and after mixing for 3 min, 120 mL of it was loaded into the still. By opening the PTFE valve (22) at the feed vessel (21), the mixture was charged into the heating chamber until the liquid completely submerged the electric heating element (1) (the liquid level should be approximately 2 cm above the immersion heater). Before starting the experiment, a check that the valves (11, 12, 15, and 16) were open and the valves (13 and 14) were closed was performed. Then, the cooling water was switched on to allow to flow through all the condensers (4, 5, and 6), and the magnetic stirrer was turned on at its maximum speed, and the liquid level in the heating chamber is checked again. The desired pressure value (30 kPa in this case) was set, the vacuum pump was switched on, and when the unit reached the pressure set point, the heating element was activated, too. The heating power was selected as a percent (from 0% to 100%) of the maximum heating power that the electric reboiler (1) can provide to the system and was increased over time. According to the procedure provided by the supplier of the unit, when 60 drops per min of condensate were observed, and the temperature detected by Pt-100 (8) remained stable for at least $10 \div 15$ min, the stationary behavior of the system was considered to be reached, and VLE was obtained. At the end, the heating element was switched off, and the unit was left to decrease in temperature until the ambient temperature was reached. Then, the unit was brought to the atmospheric pressure, and once emptied, it was filled with the second portion of the already-prepared mixture for another measurement.

The overall procedure was repeated at least two times to ensure the repeatability of the experiment and to reduce uncertainties in the measurements. The considered points were mole fractions in the liquid phase of the more volatile component equal to 0, 0.01, 0.03, 0.05, 0.1, every 0.1 for $0.1 < x < 0.9$, 0.9, 0.95, 0.97, 0.99, and 1, with more points for the mixtures richer in the pure compounds for better understanding the trend of the curve. Additional compositions were considered for the azeotropic mixture in order to better define the non-ideality characteristic of the system.

2.4. Estimation of Uncertainties

The estimation of the uncertainty is relevant for analyzing the measured experimental points. The uncertainty in T_b rises from the repeated reading of this variable with the Pt-100 (9) thermometer and can be calculated according to the methodology proposed by Taylor and Kuyatt [33]:

$$U_{rep}(T_b) = \sqrt{\frac{1}{N(N-1)} \sum_{k=1}^{N} \left(T_{b,k} - T_b^{ave}\right)^2} \quad (1)$$

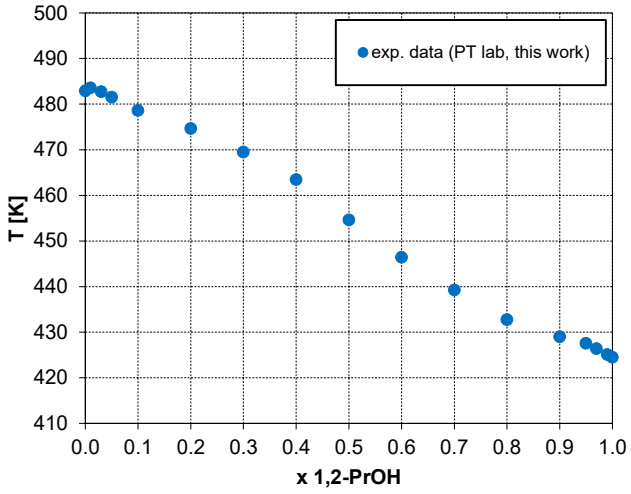
where N is the total number of T_b measurements for each blend composition.

In order to define the expanded uncertainty, $U(T_b)$, i.e., the interval about the measurement within which the value of the measurand is confidently believed to lie, the $U_{rep}(T_b)$ is multiplied by a coverage factor. By considering a coverage factor equal to 2, a 95% level of confidence for the interval is ensured [33].

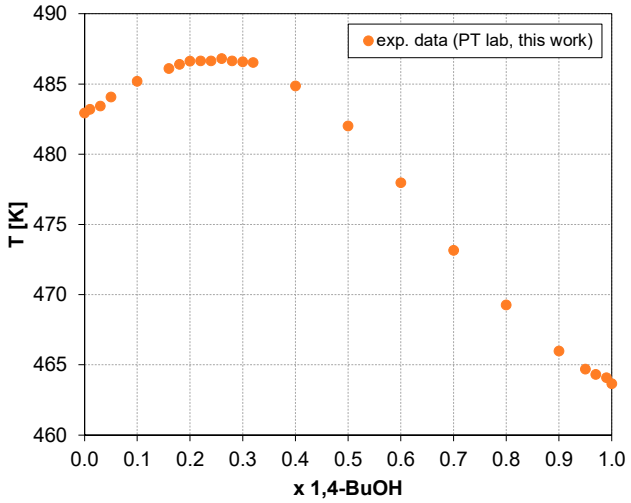
During each experiment, the pressure was kept fixed by the controller of the unit; however, being an on–off controller, small fluctuations of this variable can occur. On the basis of the measured values, estimation of the uncertainties, $U(p)$, was performed.

3. Experimental Results

The unit was previously checked by comparison of the measured data of the bubble points of pure components and mixtures as well as with azeotropes and with the literature, as detailed in Moioli et al. [31]. As reported in Figure 3 of this source, the points measured at the PT lab of Politecnico di Milano were in good agreement with the experimental points from the literature, with an error much lower than 1%.



(**a**)



(**b**)

Figure 3. Experimental bubble point data measured at PT lab of Politecnico di Milano (**a**) for the 1,2-propanediol+DBU system at 30 kPa for a mole fraction of 1,2-propanediol ranging from 0 to 1 and (**b**) for the 1,4-butanediol+DBU system at 30 kPa for a mole fraction of 1,4-butanediol ranging from 0 to 1.

The boiling temperatures obtained in this work for pure 1,2-propanediol and for pure 1,4-butanediol, the two components for which experimental data are reported in few sources ([34,35]), were in agreement with the literature values.

3.1. 1,2-Propanediol+DBU

The experimental curve for the isobaric boiling measurements at 30 kPa of the 1,2-propanediol+DBU mixture is drawn in Figure 3, and the experimental points obtained as the average of the multiple measurements are reported in Table 2. This chemical system shows a boiling behavior that is related to the composition of the loaded mixture. The mixtures with a content lower than 50% mol. in 1,2-propanediol vaporized as expected; those richer in 1,2-propanediol experienced a spray-like boiling behavior. Indeed, almost no bubbles could be detected in the system when, very close to the bubble point, the liquid phase started being crossed by a sudden formation of vapor, which was immediately able to drag the liquid phase up to the separation chamber. The Pt-100 (8) was characterized by a pulse increase in the temperature value, while the value of Pt-100 (9) decreased because of the change of the liquid level in the heating chamber, which made the temperature sensor uncovered by the liquid phase for a fraction of second. Once the liquid phase returned to the immersion heater chamber, the Pt-100 (9) temperature started to increase again, while the system could sit idle for a while without any bubble formations. However, the same spray behavior was likely to repeat itself unless a stepwise increase of the heating power was performed. Only when the boiling phenomenon and the temperature were stable was the measurement performed.

Table 2. Data of temperature and composition of the liquid phase measured at PT lab of Politecnico di Milano at a pressure of 30 kPa and related average expanded uncertainties (*U*) (a) for the system 1,2-propanediol+DBU (*x* is the mole fraction of the most volatile component, i.e., 1,2-Propandiol, in the liquid phase) and (b) for the system 1,4-butanediol+DBU (*x* is the mole fraction of the most volatile component, i.e., 1,4-butanediol, in the liquid phase).

(a)	
T_b [K]	x
424.50	1
425.11	0.99
426.41	0.97
427.56	0.95
429.01	0.9
432.74	0.8
439.24	0.7
446.44	0.6
454.63	0.5
463.48	0.4
469.51	0.3
474.71	0.2
478.63	0.1
481.55	0.05
482.73	0.03
483.59	0.01
482.94	0
The average expanded uncertainties are *U*(pressure) = 0.3 kPa; *U*(temperature) = 0.3882 K.	

Table 2. *Cont.*

(b)	
T_b [K]	**x**
463.65	1
464.08	0.99
464.31	0.97
464.69	0.95
465.98	0.9
469.26	0.8
473.15	0.7
477.96	0.6
482.00	0.5
484.86	0.4
486.58	0.3
486.63	0.2
485.19	0.1
484.07	0.0501
483.42	0.0301
483.19	0.01
482.94	0

The average expanded uncertainties are U(pressure) = 0.3 kPa; U(temperature) = 0.2506 K.

3.2. 1,4-Butanediol+DBU

The experimental curve for the isobaric boiling measurements at 30 kPa of the 1,4-butanediol+DBU mixture is reported in Figure 3, and the experimental points are detailed in Table 2.

To increase the accuracy in the definition of the azeotropic composition, more experimental points were measured for compositions of the mixture in a range of values close to the azeotropic one. The system is characterized by an azeotrope (maximum temperature) that was determined in this work for the first time, with the maximum temperature occurring for a mole fraction of 1,4-butanediol of 0.26 and a temperature equal to 486.81 K. No other sources in the literature related to DBU mention the presence of an azeotrope for this mixture. The azeotrope occurred for the mixture with 1,4-butanediol and did not occur for the mixture with 1,2-propanediol. This is related to the different shape and characteristics of the two alcohol molecules, with the 1,4-butanediol being a more linear molecule with a different affinity to the DBU molecule.

The boiling temperature of pure DBU (482.94 K) is in line with the temperature predicted by extending the Antoine equation with the adjustable parameters provided by Ostonen et al. [28] in the temperature range 375–437 K.

4. Thermodynamic Modeling

The NRTL model (Non-Random Two Liquids), developed by Renon and Prausnitz [36] and represented in Equation (2), was implemented in Aspen Plus® V14 and was used to calculate the liquid activity coefficients. It is characterized by the non-randomness parameter and can be employed for representing non-ideal systems both for VLE and LLE applications [37].

For comparison, the Wilson model [38] represented in Equation (3) and the UNIQUAC model [39] represented in Equation (4) were also used to calculate the activity coefficients for the phase equilibrium and compared to the NRTL model.

In Equation (2), the binary parameters a_{ij}, b_{ij}, c_{ij}, d_{ij}, e_{ij}, and f_{ij} can be determined from VLE and/or LLE data regression. The parameters a_{ij}, b_{ij}, e_{ij}, and f_{ij} are asymmetric, so a_{ij} may not be equal to a_{ji}, etc., but $c_{ij} = c_{ij}$, and $d_{ij} = d_{ij}$. The Aspen physical property system

has a large number of built-in binary parameters for the NRTL model, which are also used in other variants of NRTL for polymers and electrolytes, regressed from the NIST database.

In Equation (3), the binary parameters a_{ij}, b_{ij}, c_{ij}, d_{ij}, and e_{ij}, of Wilson must be determined from data regression. Parameters a_{ij}, b_{ij}, c_{ij}, d_{ij}, and e_{ij}, are asymmetric; that is, a_{ij} may not be equal to a_{ji}, etc. The same is true for UNIQUAC in Equation (4).

However, for innovative mixtures like the ones presented in this paper, there are no data available in the literature for the regression of binary interaction model parameters, so the simulator considers the mixtures of DBU and the diols to make all the relevant binary interactions parameters equal to 0 by default. The values of these parameters should be different than 0; otherwise, liquid activity coefficients equal to one are considered, as in a perfectly ideal mixture. This assumption is not acceptable for modeling purposes and should be corrected by calibrating the relevant parameters utilizing the experimental VLE data measured in this work.

$$\ln(\Upsilon_i) = \frac{\sum_j x_j \tau_{ji} G_{ji}}{\sum_k x_k G_{ki}} + \sum_j \frac{x_j G_{ij}}{\sum_k x_k G_{kj}} * \left(\tau_{ij} - \frac{\sum_m x_m \tau_{mj} G_{mj}}{\sum_k x_k G_{kj}}\right) \quad \text{for } T_{lower} \le T \le T_{upper} \tag{2}$$

where

$$G_{ij} = exp\left(-\alpha_{ij}\tau_{ij}\right)$$

$$\tau_{ij} = a_{ij} + \frac{b_{ij}}{T} + e_{ij}\ln T + f_{ij}T$$

$$a_{ij} = c_{ij} + d_{ij}(T - 273.15K)$$

$$\tau_{ii} = 0$$

$$G_{ii} = 1$$

$$\ln(\Upsilon_i) = 1 - \ln\left(\sum_j A_{ij}x_j\right) - \sum_j \frac{A_{ji}x_j}{\sum_k A_{jk}x_k} \tag{3}$$

where

$$\ln\left(A_{ij}\right) = a_{ij} + \frac{b_{ij}}{T} + c_{ij}\ln(T) + d_{ij}T + \frac{e_{ij}}{T^2}$$

$$\ln(\Upsilon_i) = \ln\left(\frac{\phi_i}{x_i}\right) + \frac{z}{2}q_i\ln\left(\frac{\theta_i}{\phi_i}\right) - q_i\prime\ln\left(t_i'\right) - q_i\prime\sum_j \frac{\theta'_j\tau_{ij}}{t'_j} + l_i + q_i\prime - \frac{\phi_i}{x_i}\sum_j x_j l_j \tag{4}$$

where

$$\theta_i = \frac{q_i x_i}{q_T}$$

$$q_T = \sum_k q_k x_k$$

$$\theta_i{}' = \frac{q'_i x_i}{q'_T}$$

$$q_T{}' = \sum_k q_k{}' x_k$$

$$\phi_i = \frac{r_i x_i}{r_T}$$

$$r_T = \sum_k r_k x_k$$

$$l_i = \frac{z}{2}(r_i - q_i) + 1 - r_i$$

$$t_i{}' = \sum_k \theta_k{}' \tau_{ki}$$

$$\tau_{ij}{}' = \exp\left(a_{ij} + \frac{b_{ij}}{T} + c_{ij}\ln(T) + d_{ij}T + \frac{e_{ij}}{T^2}\right)$$

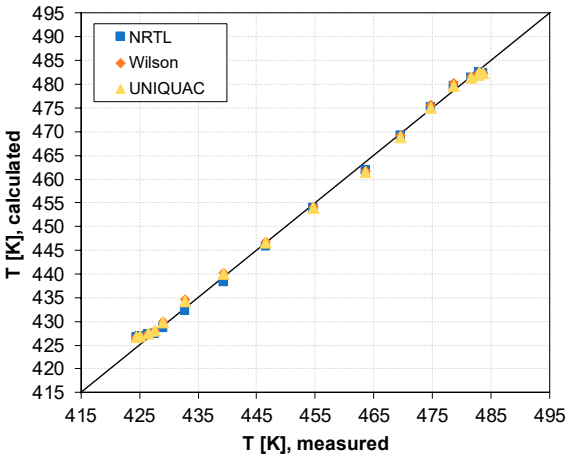
$$z = 10$$

The resulting parameters obtained with the data regression system of Aspen Plus® are reported in Table 3. The plots in Figure 4 and in Figure 5 show the accuracy of the regression, which was also confirmed by the percent average absolute deviation (AAD%), calculated in Equation (5), where n is the number of experimental points for each set of data, and reported in Table 4.

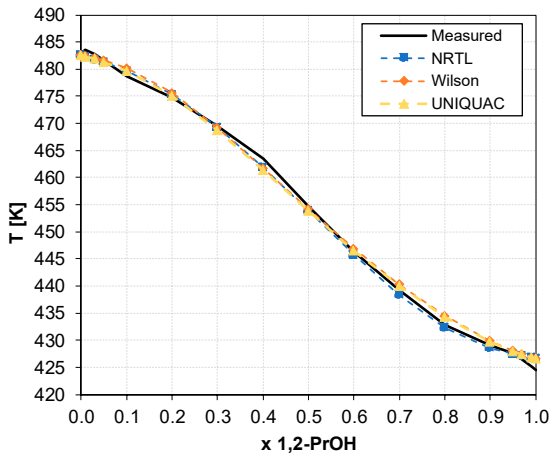
$$AAD\% = \frac{\sum_{i=1}^{n}\left|\frac{(calc\ value_i - \exp value_i)}{\exp value_i}\right|}{n} \times 100\% \quad (5)$$

Table 3. Regressed binary interaction parameters and standard deviations for the 1,4-butanediol+DBU and 1,2-propanediol+DBU systems.

	NRTL		Wilson		UNIQUAC	
Parameter	**Value [/]**	**Std. Dev.**	**Value [/]**	**Std. Dev.**	**Value [/]**	**Std. Dev.**
$a_{1,4\text{-BuOH/DBU}}$	5.059	0.440	0.481	0.009	0.678	0.002
$a_{\text{DBU/1,4-BuOH}}$	−2.523	0.033	0.861	0.292	−0.545	0.031
$a_{1,2\text{-PropOH/DBU}}$	5.067	0.034	1.006	0.002	0.644	0.001
$a_{\text{DBU/1,2-PropOH}}$	−2.641	0.183	0.536	0.057	−0.398	0.023

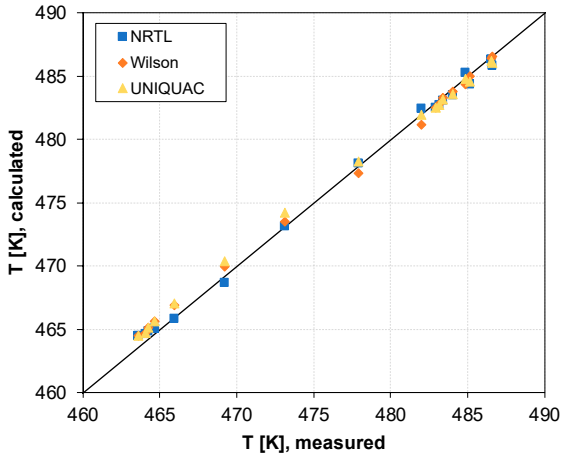


(**a**)

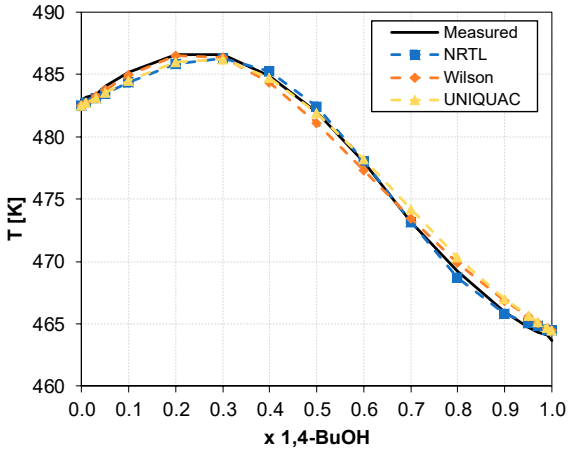


(**b**)

Figure 4. (**a**) Parity plot of the bubble point temperature and (**b**) experimental and calculated bubble points for the 1,2-propanediol+DBU mixture for a mole fraction of 1,2-propanediol ranging from 0 to 1.



(**a**)



(**b**)

Figure 5. (**a**) Parity plot of the bubble point temperature and (**b**) experimental and calculated bubble points for the 1,4-butanediol+DBU mixture for a mole fraction of 1,4-butanediol ranging from 0 to 1.

Table 4. Calculated values of AAD% for the NRTL, Wilson, and UNIQUAC methods. The NRTL model achieved the lowest deviation in both the considered mixtures.

1,4-butanediol+DBU					
NRTL		Wilson		UNIQUAC	
AAD%	0.095	AAD%	0.111	AAD%	0.125
1,2-propanediol+DBU					
NRTL		Wilson		UNIQUAC	
AAD%	0.187	AAD%	0.221	AAD%	0.212

5. Conclusions

This work is the first one reporting the experimental data of isobaric bubble points for 1,2-propanediol+DBU and 1,4-butanediol+DBU binary mixtures, which were measured at the PT lab of Politecnico di Milano (part of the Process Design and Process Thermodynamics laboratory (PD&PT lab), held by the research group GASP) at 30 kPa to address the lack of experimental data in the literature for understanding the suitability of these mixtures as possible solvents for CO_2 removal. The data were employed for the thermodynamic modelling of the binary systems, considering three different thermodynamic models (NRTL, Wilson, and UNIQUAC) and determining the interaction parameters in the simulator Aspen Plus® V14. The obtained AAD% are equal to 0.187% for the NRTL model, to 0.221% for the Wilson model, and to 0.212% for the UNIQUAC model for representing

the 1,2-propanediol+DBU mixture and equal to 0.095% for the NRTL model, to 0.111% for the Wilson model, and to 0.125% for the UNIQUAC model for representing the 1,4-butanediol+DBU mixture.

A possible future development of this work is related to the measurement of further experimental data for other systems with DBU for vapor–liquid equilibrium measurements of other binary mixtures of DBU + alcohols that are not considered at the moment to be of interest as mixtures for CO_2 removal. The possible measurements could be carried out to determine whether there is some correlation within the second alcohol in mixtures with DBU and the formation of azeotropic systems.

Author Contributions: Conceptualization, S.M., L.A.P., G.F. (Giacomo Filippini), A.R.d.A. and G.F. (Gianluca Fiori); methodology, S.M., L.A.P., G.F. (Giacomo Filippini), A.R.d.A. and G.F. (Gianluca Fiori); software, C.B. and G.F. (Giacomo Filippini); validation, C.B. and G.F. (Giacomo Filippini); formal analysis, S.M., L.A.P., G.F. (Giacomo Filippini), A.R.d.A. and G.F. (Gianluca Fiori); investigation, C.B. and V.S.; resources, L.A.P. and G.F. (Gianluca Fiori); data curation, C.B. and V.S.; writing—original draft preparation, C.B.; writing—review and editing, S.M., L.A.P., G.F. (Giacomo Filippini), A.R.d.A. and G.F. (Gianluca Fiori); visualization, S.M., L.A.P., G.F. (Giacomo Filippini), A.R.d.A. and G.F. (Gianluca Fiori); supervision, L.A.P. and G.F. (Giacomo Filippini); project administration, L.A.P. and G.F. (Gianluca Fiori); funding acquisition, L.A.P. and G.F. (Gianluca Fiori). All authors have read and agreed to the published version of the manuscript.

Funding: This research received no external funding.

Institutional Review Board Statement: Not applicable.

Informed Consent Statement: Not applicable.

Data Availability Statement: All the data are reported in the paper.

Conflicts of Interest: The authors declare no conflicts of interest.

References

1. Liu, Z.; Deng, Z.; Davies, S.; Ciais, P. Monitoring global carbon emissions in 2022. *Nat. Rev. Earth Environ.* **2023**, *4*, 205–206. [CrossRef]
2. Chao, C.; Deng, Y.; Dewil, R.; Baeyens, J.; Fan, X. Post-combustion carbon capture. *Renew. Sustain. Energy Rev.* **2021**, *138*, 110490. [CrossRef]
3. Gao, W.; Liang, S.; Wang, R.; Jiang, Q.; Zhang, Y.; Zheng, Q.; Xie, B.; Toe, C.Y.; Zhu, X.; Wang, J.; et al. Industrial carbon dioxide capture and utilization: State of the art and future challenges. *Chem. Soc. Rev.* **2020**, *23*, 8584–8686. [CrossRef]
4. Wang, R.; Zhao, H.; Wang, Y.; Qi, C.; Shihan, Z.; Li, L.W.M. Development of biphasic solvent for CO_2 capture by tailoring the polarity of amine solution. *Fuel* **2022**, *325*, 124885. [CrossRef]
5. Singh, P.; Shah, S.; Rai, S.K. Post-combustion carbon capture by polymeric membrane: A review. *Mater. Today Proc.* **2022**, *62*, 318–324. [CrossRef]
6. Raganati, F.; Miccio, F.; Ammendola, P. Adsorption of Carbon Dioxide for Post-combustion Capture: A Review. *Energy Fuels* **2021**, *35*, 12845–12868. [CrossRef]
7. Heldebrant, D.J.; Koech, P.K.; Glezakou, V.A.; Rousseau, R.; Malhotra, D.; Cantu, D.C. Water-Lean Solvents for Post-Combustion CO_2 Capture: Fundamentals, Uncertainties, Opportunities, and Outlook. *Chem. Rev.* **2017**, *117*, 9594–9624. [CrossRef] [PubMed]
8. De Guido, G.; Pellegrini, L.A. Calculation of solid-vapor equilibria for cryogenic carbon capture. *Comput. Ad Chem. Eng.* **2022**, *156*, 107569. [CrossRef]
9. IEA. *Energy Technology Perspectives 2020—Special Report on Carbon Capture Utilisation and Storage: CCUS in Clean Energy Transitions*; OECD Publishing: Paris, France, 2020; p. 171.
10. Rochelle, G.T. Amine Scrubbing for CO_2 Capture. *Science* **2009**, *325*, 1652–1654. [CrossRef]
11. Ye, Y.; Zhao, X.; Chen, J.; Fang, M. Pilot-Scale Experimental Study of a New High-Loading Absorbent for Capturing CO_2 from Flue Gas. *Processes* **2022**, *10*, 599. [CrossRef]
12. Kladkaew, N.; Idem, R.; Tontiwachwuthikul, P.; Saiwan, C. Corrosion Behavior of Carbon Steel in the Monoethanolamine-H_2O-CO_2-O_2-SO_2 System: Products, Reaction Pathways, and Kinetics. *Ind. Eng. Chem. Res.* **2009**, *48*, 10169–10179. [CrossRef]

13. Davis, J.; Rochelle, G. Thermal degradation of monoethanolamine at stripper conditions. *Energy Procedia* **2009**, *1*, 327–333. [CrossRef]
14. Novitsky, E.G.; Grushevenko, E.A.; Borisov, I.L.; Anokhina, T.S.; Bazhenov, S.D. Monoethanolamine (MEA) Degradation: Influence on the Electrodialysis Treatment of MEA-Absorbent. *Membranes* **2023**, *13*, 491. [CrossRef]
15. Jessop, P.G.; Heldebrant, D.J.; Li, X.; Eckert, C.A.; Liotta, C.L. Green chemistry: Reversible nonpolari-to-polar solvent. *Nature* **2005**, *436*, 1102. [CrossRef]
16. Heldebrant, D.J.; Yonker, C.R.; Jessop, P.G.; Phan, L. CO_2-binding organic liquids (CO_2BOLs) for post-combustion CO_2 capture. *Energy Procedia* **2009**, *1*, 1187–1195. [CrossRef]
17. Lide, D.R. *Handbook of Chemistry and Physics*; CRC Press: Boca Raton, FL, USA, 2003.
18. Heldebrant, D.J.; Yonker, C.R.; Jessop, P.G.; Phan, L. Organic liquid CO_2 capture agents with high gravimetric CO_2 capacity. *Energy Environ. Sci.* **2008**, *1*, 487–493. [CrossRef]
19. Heldebrant, D.J.; Koech, P.K.; Ang, M.T.C.; Liang, C.; Rainbolt, J.E.; Yonker, C.R.; Jessop, P.G. Reversible zwitterionic liquids, the reaction of alkanol guanidines, alkanol amidines, and diamines with CO_2. *Green Chem.* **2010**, *12*, 713–721. [CrossRef]
20. Wanderley, R.R.; Høisæter, K.H.; Knuutila, H.K. Signs of alkylcarbonate formation in water-lean solvents: VLE-based understanding of pKa and pKs effects. *Int. J. Greenh. Gas Control* **2021**, *109*, 103398. [CrossRef]
21. Mathias, P.M.; Afshar, K.; Zheng, F.; Bearden, M.D.; Freeman, C.J.; Andrea, T.; Koech, P.K.; Kutnyakov, I.; Zwoster, A.; Smith, A.R.; et al. Improving the regeneration of CO_2-binding organic liquids with a polarity change. *Energy Environ. Sci.* **2013**, *6*, 2233–2242. [CrossRef]
22. Zhu, X.; Lu, H.; Wu, K.; Zhu, Y.; Liu, Y.; Liu, C.; Liang, B. DBU-glycerol solution: A CO_2 absorbent with high desorption ratio and low regeneration energy. *Environ. Sci. Technol.* **2020**, *54*, 7570–7578. [CrossRef]
23. Duan, H.; Zhu, K.; Lu, H.; Liu, C.; Wu, K.; Liu, Y.; Liang, B. CO_2 absorption performance in a rotating disk reactor using DBU-glycerol as solvent. *Chin. J. Chem. Eng.* **2020**, *28*, 104–113. [CrossRef]
24. Lin, S. Study on Thermodynamical Properties of 1,8-diazabicyclo [5.4.0 undec-7-ene (DBU)-glycerol and CO_2-DBU-glycerol Solutions. Master's Thesis, Sichuan University, Chengdu, China, 2018.
25. Li, Y.; Lu, H.; Liu, Y.; Wu, K.; Zhu, Y.; Liang, B. CO_2 absorption and desorption enhancement by nano-SiO_2 in DBU-glycerol solution with high viscosity. *Sep. Purif. Technol.* **2023**, *309*, 122983. [CrossRef]
26. Liu, F.; Jing, G.; Lv, B.; Zhou, Z. High regeneration efficiency and low viscosity of CO_2 capture in a switchable ionic liquid activated by 2-amino-2-methyl-1-propanol. *Int. J. Greenh. Gas Control* **2017**, *60*, 162–171. [CrossRef]
27. Hedayati, A.; Feyzi, F. CO_2-binding organic liquids for high pressure CO_2 absorption: Statistica mixture design approach and thermodynamic modeling of CO_2 solubility using LJ-Global TPT2 EoS. *J. Mol. Liq.* **2021**, *337*, 116396. [CrossRef]
28. Ostonen, A.; Uusi-Kyyny, P.; Pakkanen, M.; Alopaeus, V. Dew points of pure DBN and DBU and vapor-liquid equilibria of water + DBN and water + DBU systems for cellulose solvent recycling. *Fluid. Phase Equilibria* **2016**, *408*, 79–87. [CrossRef]
29. Lipkind, D.; Rath, N.; Chickos, J.S.; Pozdeev, V.A.; Verevkin, S.P. The Vaporization Enthalpies of 2- and 4-(N,N-Dimethylamino)pyridine, 1,5-Diazabicyclo [4.3.0]non-5-ene, 1,8-Diazabicyclo[5.4.0]undec-7-ene, Imidazo[1,2-a]pyridine and 1,2,4-Triazolo[1,5-a]pyrimidine by Correlation-Gas Chromatography. *J. Phys. Chem. B* **2011**, *115*, 8785–8796. [CrossRef] [PubMed]
30. Boddu, S.K.; Rehman, N.U.; Mohanta, T.K.; Majhi, A.; Avula, S.K.; Al-Harrasi, A. A review on DBU-mediated organic transformations. *Green Chem. Lett. Rev.* **2022**, *15*, 765–795. [CrossRef]
31. Moioli, S.; De Guido, G.; Gilardi, M.; Pellegrini, L.A.; Bonalumi, D.; Lozza, G. Isobaric Vapor-Liquid Equilibrium Data for the Isopropanol-Water System. *J. Chem. Eng. Data* **2021**, *66*, 4148–4158. [CrossRef]
32. De Guido, G.; Moioli, S.; Gilardi, M.; Giudici, F.; Pellegrini, L. Downstream processing of butanol produced by fermentation: Thermodynamic measurements and modelling. *Chem. Eng. Trans.* **2022**, *92*, 625–630.
33. Spatolisano, E.; Barbieri, C.; Pellegrini, L.; Moioli, S. Thermodynamic study and simulation of the process of separation of the IPA+water mixture by heterogeneous azeotropic distillation. In *Computer-Aided Chemical Engineering*; Elsevier: Amsterdam, The Netherlands, 2023; pp. 2507–2512.
34. Taylor, B.N.; Kuyatt, C.E. *Guidelines for Evaluating and Expressing the Uncertainty of NIST Measurement Results*; NIST Technical Note 1297; National Institute of Standards and Technology: Gaithersburg, MD, USA, 1994.
35. Mathuni, T.; Kim, J.-I.; Park, S.-J. Phase Equilibrium and Physical Properties for the Purification of Propylene Carbonate (PC) and y-Butyrolactone (GBL). *J. Chem. Eng. Data* **2011**, *56*, 89–96. [CrossRef]
36. Gardner, P.J.; Hussain, K.S. The Standard Enthalpies of Formation of Some Aliphatic Diols. *J. Chem. Thermodyn.* **1972**, *4*, 819–827. [CrossRef]
37. Renon, H.; Prausnitz, J.M. Local Compositions in Thermodynamic Excesss Functions for Liquid Mixtures. *AIChE J.* **1968**, *14*, 135–144. [CrossRef]

38. Luyben, W.L.; Chien, I.L. *Design and Control of Distillation Systems for Separating Azeotropes*; John Wiley & Sons: Hoboken, NJ, USA, 2011.
39. Abrams, D.S.; Prausnitz, J.M. Statistical Thermodynamics of liquid mixtures: A new expression for the Excess Gibbs Energy of Partly or Completely Miscible Systems. *AIChE J.* **1964**, *86*, 127. [CrossRef]

Disclaimer/Publisher's Note: The statements, opinions and data contained in all publications are solely those of the individual author(s) and contributor(s) and not of MDPI and/or the editor(s). MDPI and/or the editor(s) disclaim responsibility for any injury to people or property resulting from any ideas, methods, instructions or products referred to in the content.